Marine Micropaleontology 206 (2026) 102591

Contents lists available at ScienceDirect

Marine Micropaleontology

journal homepage: www.elsevier.com/locate/marmicro

Research paper

Modern Southern Ocean sea ice environments are reflected in eukaryotic DNA from the sea floor☆

Nele M. Vollmar [a,b,*], Agnes K.M. Weiner [a], Katja Häkli [c,g], Miriam I. Brandt [c], Juliane Müller [d], Oliver Esper [d], Thomas G. Dahlgren [c,e], Claire S. Allen [f], Tristan Cordier [a], Stijn De Schepper [a,b]

[a] NORCE Climate and Environment, NORCE Research AS and Bjerknes Centre for Climate Research, Bergen, Norway
[b] Department of Earth Science, University of Bergen, Bergen, Norway
[c] NORCE Climate and Environment, NORCE Research AS, Bergen, Norway
[d] Alfred Wegener Institute, Helmholtz Centre for Polar and Marine Research, Bremerhaven, Germany
[e] Department of Marine Sciences, University of Gothenburg, Gothenburg, Sweden
[f] British Antarctic Survey, Cambridge, United Kingdom
[g] now at The Arctic University Museum of Norway, UiT - The Arctic University of Norway, Norway

ARTICLE INFO

Keywords:
Sedimentary DNA
Weddell Sea
Southern Ocean
Sea ice proxy
Metabarcoding

ABSTRACT

In the Southern Ocean, reconstructions of past sea ice conditions remain challenging because of limited proxy and calibration approaches. Sedimentary DNA can complement the available proxies for reconstructing past sea ice environments and thereby provide additional and/or new insights into past regional and global climate evolution. However, its application requires an established relationship between seafloor surface sediment DNA composition and modern sea ice conditions. Here we show, using a metabarcoding approach (V9 18S rRNA) on 45 surface sediment samples from the Weddell Sea, that contemporary sea ice environments are reflected in the sedimentary DNA community composition. Our results further reveal that sea ice concentration and water depth have a significant effect on community variance. Most relevant for paleoenvironmental applications, our data indicates a dominance in relative abundance of Chaetocerotaceae diatom DNA in polynya-related regions, agreeing with previous diatom microfossil assemblage studies. These results establish this family as a robust molecular proxy for these productive environments. We also show that planktic taxa were more influenced by sea ice concentration than benthic taxa, indicating that focusing on planktic taxa for sea ice reconstructions in sedimentary ancient DNA may be more effective. We conclude that an environmental genomics approach can complement and extend existing proxy records, especially for organisms without a fossil record and areas with limited conventional proxy data.

1. Introduction

Sea ice is a critical part of polar and global climate dynamics via its role in deep-water formation, the albedo effect, buttressing of ice shelves, and as ecological habitat (Crosta et al., 2022; Koch et al., 2023; Massom et al., 2018; Roach and Meier, 2025). In order to fully understand the role of sea ice dynamics in the climate system, it is imperative to look at the evolution of sea ice on timescales beyond the satellite era. Observations from space document the evolution of sea ice only since the late 1970s, limiting our understanding of long-term trends in sea ice extent, concentration or thickness, and ultimately the drivers of such change. Information about long-term climate trends and sea ice evolution can be obtained from marine sediments, which are an archive for past and present climate and environmental conditions. Sediments contain (traces of) organisms or their biogeochemical signatures (e.g. biomarkers, DNA), which can be exploited as proxies for e.g. sea surface temperature (SST) or sea ice. Before proxies are applied to the geological record (e.g. Crosta et al., 2022; Vorrath et al., 2020), they need calibration (e.g Cárdenas et al., 2019; Lamping et al., 2021). For the Southern Ocean, this has been done for diatom assemblages and biomarkers, but not for sedimentary DNA which has been suggested as a new proxy for sea ice reconstruction in the Arctic (e.g. De Schepper

☆ This article is part of a Special issue entitled: 'Marine sedaDNA' published in Marine Micropaleontology.

* Corresponding author at: NORCE Climate and Environment, NORCE Research AS and Bjerknes Centre for Climate Research, Bergen, Norway.
E-mail addresses: nevo@norceresearch.no, nvollmar@uni-bremen.de (N.M. Vollmar).

https://doi.org/10.1016/j.marmicro.2026.102591
Received 3 December 2025; Received in revised form 22 May 2026; Accepted 28 May 2026
Available online 12 June 2026

et al., 2019; Mayers et al., 2026).

Over the last decade, the analysis of DNA extracted from environmental samples such as marine sediments has emerged as a research field driven by advances in high throughput sequencing technologies (Hugerth and Andersson, 2017; Taberlet et al., 2012). Sedimentary DNA is a complex mixture of intracellular DNA (enclosed in intact cells from living or dead organisms) and extracellular DNA (released from e.g. lysed or degraded cells) originating from various living or dead organisms from microorganisms to large size animals (Taberlet et al., 2012, 2018). It is a mixture of DNA originating from two sources: allochthonous DNA transported to the sea floor, including sinking planktic material from the overlying waters and ice, and autochthonous DNA from living and dead epi- and infaunal benthic organisms living in the sediment (Taberlet et al., 2012; Torti et al., 2015). Compared to conventional paleoceanographic proxies such as microfossils or biomarkers (Coolen and Gibson, 2009), sedimentary DNA holds information about entire biological communities, including organisms that do not leave behind a test or cyst, and it can thus greatly complement established proxies. Metabarcoding, a DNA based method targeting taxonomically-informative genes, can be used to screen contemporary community composition in seafloor surface sediments (e.g. Cordier et al., 2022; Geraldi et al., 2024) and, when applied to older sediment layers, can be used to reconstruct past community compositions with sedimentary ancient DNA (sedaDNA) (e.g. Armbrecht, 2020; De Schepper et al., 2019; Ellegaard et al., 2020; Epp et al., 2019).

SedaDNA holds great potential as a new paleoceanographic proxy (Armbrecht, 2020; De Schepper et al., 2019; Morard et al., 2017). To harness its potential, we first need to assess whether the composition of contemporary sedimentary DNA is imprinted by current environmental conditions. So far, there is a limited number of studies applying sedimentary DNA as an environmental indicator in polar regions (e.g. Geraldi et al., 2024; Ørberg et al., 2022; Pawlowski et al., 2011). Although the biodiversity of Southern Ocean pelagic ecosystems has been documented with metabarcoding (Clarke et al., 2019; Flegontova et al., 2023), there exist very few comprehensive assessments of biodiversity in seafloor sediments using metabarcoding in the Southern Ocean (e.g. Learman et al., 2016; but see Brandt et al. (2007) and Grimes et al. (2025) for studies based on photo-transects and morphotaxonomy). To our knowledge no evaluation of the potential of sedimentary DNA as sea ice proxy exists for this region.

The Weddell Sea in the Southern Ocean represents a natural laboratory for investigating sea ice - sedimentary DNA relationships. The region encompasses diverse sea ice regimes from perennial to seasonal sea ice environments as well as polynya-related environments (i.e. persistent windows of open water within ice-covered ocean) within a single oceanographic system. Changes in sea ice conditions, and consequently also in primary production in the upper ocean, directly affect planktic community composition and indirectly also benthic biodiversity via organic matter exported to the seafloor via the biological carbon pump (De La Rocha and Passow, 2007; Ducklow et al., 2001; Iversen, 2023), although the responses act on different timescales. Therefore, it can be hypothesized that the planktic community compartment retrieved in sedimentary DNA may more strongly reflect surface ocean conditions than the benthic compartment.

In this study we investigated surface sediment samples from 45 stations across different environments in the Weddell Sea and Drake Passage using metabarcoding of the V9 hypervariable region of the small-subunit ribosomal RNA gene (18S V9). In the first instance, we assessed whether eukaryote communities detected in environmental DNA from surface sediments (hereafter sedimentary DNA communities or eukaryotic communities) can differentiate modern sea ice environments (open water, seasonal sea ice, polynyas and perennial sea ice). We then evaluated whether the planktic community signal in sediment material was more affected by sea ice conditions than the whole community.

2. Study region and sea ice environments

Our study region, the Weddell Sea, one of three major oceanic regions in the Southern Ocean (Stark et al., 2019), is situated east of the Antarctic Peninsula and bordered by the Eastern and Western Antarctic Ice Sheets. It extends from the Polar Front in the Drake Passage in the northwest to the South Sandwich Arch in the northeastern Scotia Sea, and from the Rønne Basin in the southwestern Weddell Sea to the front of the Ekstrøm iceshelf in the southeastern Weddell Sea (Fig. 1). To the south, the West Antarctic Ice Sheet extends into the Weddell Sea via the Larsen and Rønne ice shelves, while to the southeast and east, the East Antarctic Ice Sheet protrudes into the Weddell Sea with the Filchner, Brunt and Riiser-Larsen ice shelves (Anderson, 1993; Stark et al., 2019).

The northern extent of our study area (Fig. 1) is defined by the Antarctic Circumpolar Current, driven by strong eastward winds and shaped by seafloor bathymetry (Klinck and Nowlin, 2001). The Antarctic Circumpolar Current consists of three major fronts — the Sub Antarctic Front, Polar Front and the Southern Antarctic Circumpolar Current Front, each characterized by sharp changes in water properties (Orsi et al., 1995; Sokolov and Rintoul, 2009; Stark et al., 2019). In the Drake Passage, one of the Antarctic Circumpolar Current's narrowest flowthroughs, these fronts compress into a relatively small region, creating large environmental gradients (Park et al., 2019). The strong currents limit northward sea ice expansion, particularly in the southern Drake Passage (Meier et al., 2021), resulting in largely sea ice-free conditions. This area generally has a low productivity because of iron-limitations but can host phytoplankton blooms related to upwelling (Deppeler and Davidson, 2017).

The Weddell Sea hosts three primary sea ice regimes with distinct ecological characteristics: regions with perennial sea ice, seasonal sea ice and polynyas. Perennial sea ice is most prevalent over the continental shelf, where it persists over multiple melting seasons. Stable conditions with low light availability and a cold water column host highly specialized and cold adapted organisms. High nutrient concentrations and iron supply from upwelling circumpolar deepwater, basal shelf melting and coastal sediments (Deppeler and Davidson, 2017) make these regions productive as soon as there is enough light available. Seasonal sea ice covers the Weddell Sea basin adjacent to the continental shelf and supports high primary production during the ice-free months (Deppeler and Davidson, 2017). Polynyas occur commonly in relatively shallow regions close to the coast or ice shelves. Here, open water occurs when one would normally expect sea-ice cover (Arrigo and van Dijken, 2003). Coastal polynyas form due to wind or current stress and are areas of continuous ice formation and export (Morales Maqueda et al., 2004), that contribute to Antarctic Bottom Water formation (Kusahara et al., 2017; Morales Maqueda et al., 2004). These areas are hot spots for primary production in summer, with high sedimentation rates of organic material, followed by nutrient depletion in the surface (Arrigo and van Dijken, 2003). The high primary production results in a higher concentration of higher trophic level organisms as well as diverse benthic communities (Arrigo and van Dijken, 2003).

3. Material and methods

3.1. Surface sediment collection

Surface sediments were collected using multicorers (MUC) or boxcorers during expeditions PS61 (ANT-XIX/4, Fütterer et al., 2003), PS97 (Lamy, 2016), PS111 (Schröder, 2018), PS118 (Dorschel, 2019) with RV Polarstern, and expeditions JR244 (Larter et al., 2011) and JR17003a (Linse, K., scientists of Larsen-C Benthos, February–March 2018, 2026) with RRS James Clark Ross. Details on sampling locations can be found in Fig. 1 and Appendix Table A.1. The boxcores were subsampled on board using pushcores. These subcores and all MUCs were frozen on board (−20 °C), transported back to either the Alfred Wegener Institute in Bremerhaven, Germany, or the British Antarctic

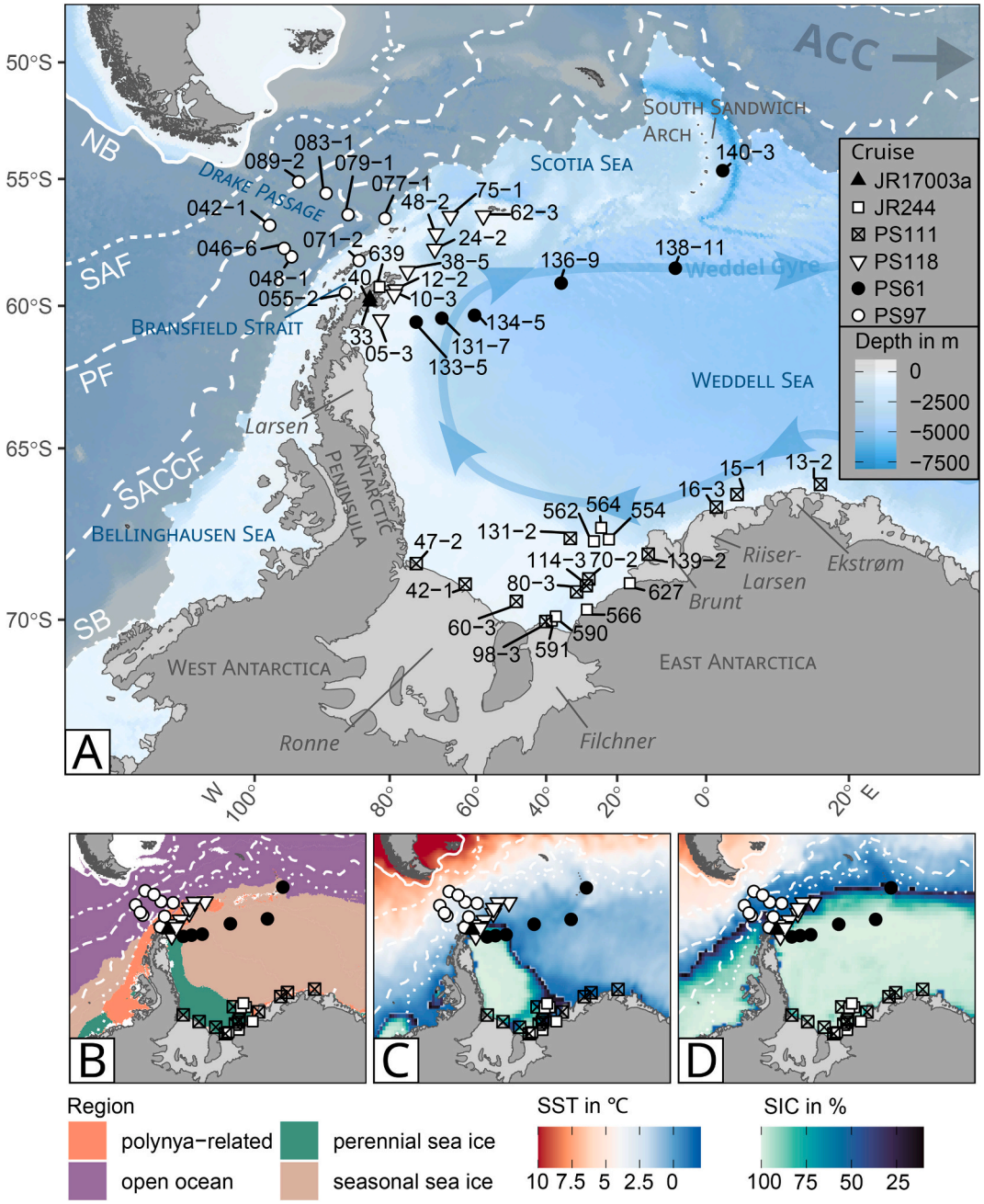

Fig. 1. A: Study area and bathymetry in the Drake Passage and Weddell Sea. Labelled points indicate sampling stations with different shapes for each cruise (Appendix Table A.1). Bathymetry from GEBCO Bathymetric Compilation Group (2023), overlain with the Antarctic Circumpolar Current (ACC) in transparent grey. White dashed lines depict the average positions of the ACC fronts after Park et al. (2019); Northern Boundary (NB), Sub Antarctic Front (SAF), Polar Front (PF), Southern Antarctic Circumpolar Current Front (SACCF), Southern Boundary (SB). Coastal and (shelf) ice outline from SCAR Antarctic Digital Database (ADD) Version 7.0, retrieved via R package SOmap version 0.6.2.9005 Maschette et al. (2019). B: Sea ice environments (regions) simplified after Raymond (2014), Appendix Table B.2. C: Summer (February 2018) sea surface temperature (SST) overlain by sea ice concentration (SIC, values below 0.1 not shown). D: Winter (August 2018) SST overlain by SIC (values below 0.1 not shown). SST from NOAA/NCEI 1/4 Degree Daily Optimum Interpolation Sea Surface Temperature (OISST) Analysis, Version 2.1 (Huang et al., 2021) and SIC from OAA/NSIDC Climate Data Record of Passive Microwave Monthly Southern Hemisphere Sea Ice Concentration (Meier et al., 2021).

Survey in Cambridge, UK, where they were stored frozen (−20 °C). Surface sediment samples from cruises JR17003a and PS61 were directly collected onboard, stored in 2 mL tubes, and frozen at −80 °C until further processing at our ancient DNA laboratory in Bergen, Norway.

To minimize contamination risk, we implemented strict sediment sampling protocols. We processed all cores at the respective institutes using appropriate personal protective equipment (PPE). Work areas were thoroughly cleaned with 10% bleach or Decon 90 (Decon Laboratories Limited) and Chemgene™ HLD4L (Medimark International™) before processing of each core. Sampling controls, consisting of sterile tubes with MilliQ water, were taken for every day in the lab, placed with lids open in the sampling area, and later pooled into three sampling control pools (one pool per sampling event). These sampling controls were later subjected to the same DNA extraction and polymerase chain reaction (PCR) amplification as the sediment samples to assess potential

contamination (Section 3.2).

Cores were thawed at room temperature, and any ice or liquid present on the sediment surface was removed using sterile equipment. When cores were still partially frozen, we sliced the uppermost cm (0–1 cm) off each core (1–2 cm for PS118/12–2, PS118/48–2, PS118–62-3; 0–2 cm for PS111/98–3; 0–0.5 cm for PS97/071–2, PS97/089–2, PS97/077–1, PS97/042–1) using a clean sharp knife and a clean spatula. From each slice, we transferred the inner part of the sediment slice using a sterile spoon into a labelled sterile 50 mL falcon tube. If cores were fully thawed, we used a spoon to collect the inner part of the upper 1 cm. Falcon tubes were frozen immediately at −20 °C and remained so during transport to and storage at the ancient DNA laboratory in Bergen until further processing.

For total organic carbon (TOC) and diatom count analysis, the rim of the upper 1 cm of sediment was sampled into a labelled sterile Whirl-Pak®, avoiding the outmost of the sediment core in contact with the liner.

3.2. DNA extraction and metabarcoding workflow

Sediment was thawed at room temperature and 0.25 g ±10% of sediment was subsampled for extraction with the 'combined' extraction protocol from Armbrecht et al. (2020) in the ancient DNA laboratory at NORCE Research AS in Bergen. Two subsampling controls were taken using 200 μL DNAse free water in open 1.5 mL microtubes. Extractions were performed in batches of twelve samples and were semi-randomized so that each extraction batch comprised samples from several cruises. Four extraction controls were taken in total, across all extraction rounds, using 250 μL DNAse free water instead of sediment. We processed all controls, including the sampling control pools (see 3.1), alongside sediment samples throughout the full workflow. DNA concentrations in extracts were measured with a Qubit™ 4 Fluorometer using the dsDNA Quantification Assay Kits (Thermo Fisher Scientific) and extracts were stored at −20 °C until amplification by PCR.

We PCR-amplified the 18S rRNA V9 region, a ~ 130 bp long fragment specific to eukaryotes but also capturing some prokaryotes using the universal forward (1389F, 5'-TTGTACACACCGCCC-3′) and eukaryote-specific reverse (1510R, 5'-CCTTCYGCAGGTTCACCTAC-3′) primer (Amaral-Zettler et al., 2009). Tag-encoded versions of the primer pair with unique 8-nucleotide tags were used to multiplex up to 48 individual reactions and two PCR negative controls into a single sequencing library. Each DNA extract was amplified in triplicate reactions with unique tagged primer combinations, resulting in three technical replicates per sediment sample. PCR amplifications were performed in 25 μL total volume using 17.9 μL of ultrapure water, 2.5 μL of 10× PCR Buffer II (AmpliTaq Gold™), 1.5 μL MgCl2 (25 mM), 0.5 μL dNTPs (10 mM), 0.5 μL bovine serum albumin (20 mg/mL), 0.1 μL AmpliTaq Gold™ DNA polymerase (5 U/μL, all chemicals from Thermo Fisher Scientific), 0.5 μL tagged forward primer (10 μM), 0.5 μL tagged reverse primer (10 μM), and 1 μL of DNA template. Thermocycling conditions were as follows: initial denaturation at 95 °C for 5 min, then 34 cycles of denaturation at 95 °C for 30s, annealing at 57 °C for 45 s, and elongation at 72 °C for 45 s; followed by a final extension at 72 °C for 5 min. Success of PCR amplifications and concentration of the target fragment in each PCR product were estimated using high-sensitivity capillary electrophoresis (QIAxcel Connect System, QIAGEN®).

The 50 PCR products (48 samples and two PCR controls) corresponding to one sequencing library were pooled equimolarly, aiming for 25 ng per sample and adding the full volume of a PCR product when this amount could not be reached. Each of the six resulting pools was purified with the Roche High Pure PCR Product Purification Kit Roche following manufacturer instructions. The DNA concentration and nucleic acid purity in the pools were quantified using a NanoDrop™ One Spectrophotometer (Thermo Fisher Scientific™). The purification was repeated for all pools because of a low 260/230 ratio below 0.65 after the first round of purification. The purified pools were then prepared as sequencing libraries using the Illumina TruSeq™ DNA PCR-free Library Preparation Kit, omitting the fragmentation step. Libraries were sequenced at the Norwegian Sequencing Centre in Oslo on an Illumina NovaSeq 6000 platform, using a SP flowcell with 150 bp paired end reads and v1.5 reagents.

3.3. Bioinformatic processing and quality control

Raw sequencing reads were demultiplexed to assign sequences to their original PCR reaction based on their unique primer tags. Processing of the sequencing data was done on an Rstudio server (R version 4.0.4, 2021–0215). The fastqUtils R package v.0.1.0 commit b1aa08b (Cordier, 2024) was used to demultiplex the reads (function demultRun) by screening for specific combinations of tagged primers associated to individual PCR reactions (zero mismatches allowed in the tagged primers), and accounting for mixed orientations of the reads due the PCR-free library preparation protocol. The output of this step was two files for each of the R1 and R2 files (i.e. forward and reverse from the R1 fastq, and forward and reverse from the R2 fastq). For deposition in the European Nucleotide Archive (ENA) under the accession number PRJEB104882, we demultiplexed sequencing data in mixed orientation (one file per R1 and R2) using fastqUtils R package v.0.1.0 commit b60c307 (function demultiplexDoublePairedforENA). Demultiplexed reads of each sequencing library were then denoised using the DADA2 pipeline v.1.18.0 (Callahan et al., 2016) to produce amplicon sequence variants (ASVs) via the function dada2workflow4files of the fastqUtils package. Reads were quality filtered using the filterAndTrim function of DADA2 (minimum sequence length 60 nt, maxEE = 2) and PCR reactions with less than 100 reads were removed. The DADA2 workflow was followed on each of the four fastq files of each PCR reaction, i.e. error modeling (learnErrors function), dereplication (derepFastq function), denoising (dada function), re-orienting the reads, and merging pairs or reads from overlapping forward and reverse reads (mergePairs function) using the "trimOverhang" option to make sure that primers are trimmed from the resulting assembly. ASV tables were produced for each library and then merged together (mergeSequenceTables function). ASVs that still contained traces of the primers were removed, and chimeras were removed (removeBimeraDenovo function, default settings).

ASVs were taxonomically assigned using SLIM's "assignment-fasta-vsearch" module (Dufresne et al., 2019) with the PR2 database version 5.0.0 (Guillou et al., 2013) as reference, applying a minimum similarity of 85%, a direct acceptance threshold of 0.99, and 3 matches to be used for assigning a consensual taxonomic rank annotation.

All following data processing and analysis were performed using R Statistical Software (v4.3.2; R Core Team, 2023) unless specified otherwise. We used the package metabaR version 1.0.0 (Zinger et al., 2021) for handling of metabarcoding data.

Contaminants were identified and partially or completely removed using the SCRuB package version 0.0.1 (Austin et al., 2023) with serial decontamination for every type of control in the order: sampling, subsampling, extraction and finally PCR control. SCRuB is assuming that reads in controls stem from contamination or well-to-well leakage. For every step it therefore removes reads from the corresponding control and partially or completely removes reads identified as contaminants from samples (see Appendix F; see Austin et al., 2023 for details). The output of each decontamination step was the input for the next decontamination step. After decontamination a principal coordinates analysis (PCoA) ordination based on Bray-Curtis dissimilarity was conducted and visually compared to a PCoA ordination of the dataset before decontaminating to confirm that decontamination did not alter the main structure of eukaryotic communities.

We removed ASVs assigned to bacteria, archaea, and unassigned ASVs shorter than 116 bp, that may correspond to unassigned prokaryotes (i.e. 16S V9 is consistently around 105 bp for bacteria and around 95 bp for archaea, whereas 18S V9 is consistently around 130 bp for eukaryotes). ASVs matching plastid reference sequences (e.g.

chloroplastic SSU) were discarded. Finally, we discarded PCR replicates for which we recovered less than 20,000 reads.

We then assigned each ASV to a planktic or benthic habitat by matching their 18S V9 sequences to a list of planktic and benthic ASVs curated from global-scale metabarcoding surveys (Cordier et al., 2022) and augmented with plankton samples collected along the water column in the Weddell Sea (Flegontova et al., 2023). Any ASV that had no exact match in this curated list of ASVs and that was exclusively found in sediment samples of this study was considered benthic (as in Cordier et al., 2022).

Prior to analysis of taxonomic composition, we aggregated replicates per sample by summing up reads for each ASV. Because of the compositional nature of metabarcoding data we report relative abundances of a given taxonomic rank (e.g. ASV, family, subdivision). Those were calculated by dividing the absolute number of reads of this taxonomic rank by the total number of reads in the respective sample.

3.4. Regional classification

Stations with similar broad ecological characteristics were grouped into four discrete sea ice environments (i.e. open ocean, seasonal sea ice, perennial sea ice and polynya regions; see Appendix Tables A.1 and B.2). We based these on the pelagic regionalisation of Raymond (2014), a classification based on summer climatological SST, water depths and the proportion of time covered by a sea ice concentration of $\geq$85% between January 2003 and December 2009 (Mormède et al., 2014). The regionalisation was accessed using the R package quantarcticR version 0.1.4 (Fitter et al., 2025) and sampling stations were spatially joined with pelagic region polygons using sf::st_join. Six stations required special treatment because of their proximity to region boundaries. For two stations (JR17003a/40 and JR244/639), a 14 km buffer was used to extract the closest corresponding region. For four stations the buffer resulted in two possible region assignments; in these cases, surrounding cluster patterns were examined to determine the best fit (PS111/139-2, JR244/566, JR244/627, PS97/071-2).

Our stations fell into 11 of the original 16 clusters from Raymond (2014). We simplified the most similar regions into four broader pelagic regions representing different sea ice environments (Appendix Table B.2). Those encompass similar ecological characteristics regarding summer SST, water depth and sea ice persistence, therefore capturing the main environmental gradients. The "polynya-related region" merges polynya margins, polynyas and regions around polynyas. The "perennial sea-ice region" merges shallow shelf areas with a sea ice coverage of >25% as well as shelf areas with almost perennial sea ice cover. The "seasonal sea ice region" combines several sea ice zones with increasing ice cover. The "open ocean region" is merged from deep oceanic water clusters. That way we created ecologically meaningful groupings and obtained a reasonable number of stations per group.

3.5. Environmental variables

Sea ice concentration (SIC) was extracted for each station to characterize long-term sea ice conditions and seasonal variability. SIC data beginning with the start of observations (November 1978) to the month of sampling was extracted from the 25 km2 NOAA/NSIDC climate data record of passive microwave SIC G02202 version 4 (Meier et al., 2021). The extract function from the raster R package version 3.6-26 (Hijmans, 2023) was used with the "simple" method for most stations (extracting the SIC value for the exact station position), the "bilinear" method for three stations (JR244/566, JR244/639, JR244/627; interpolating the SIC value from the four nearest raster cells) and with the buffer option set to a radius of 35 km for four stations where it was necessary because of missing data close to the coast (JR17003a/33, JR17003a/40, JR244/591, PS111/98-3; extracting the available SIC values from all cells in a radius of 35 km around the station location and taking their average). For each station, averages and standard deviations were calculated over the entire period, from Nov. 1978 until the sampling month (SIC average and SIC variability, respectively), and separately for each season (seasonal SIC average and seasonal SIC variability, respectively): summer (December–February), Fall (March–May), Winter (June–August) and Spring (September–November).

Monthly mean SST data was extracted from NOAA/NCEI 1/4 Degree Daily Optimum Interpolation Analysis (OISST) v2.1 (Huang et al., 2021) from the beginning of observations (September 1981) until the month of sampling in the same way as for SIC but using the "simple" method for all stations.

The distance to the ice shelf was retrieved using the function dist2land from the ggOceanMaps R package v.2.2.0 (Vihtakari, 2022) with the station coordinates and the "ant_coast_ice" shape (Fitter et al., 2025) from the SOmap R package v. 0.5.0 (Maschette et al., 2019). Distance to both, the Antarctic and American coast was retrieved the same way, with "ant_coast_land" for the Antarctic coastline and "GSHHS_i_L1" for the South American coast.

To avoid multicolinearity of variables in the statistical analyses, we selected environmental parameters through correlation testing and variance inflation factor assessment. We considered the following environmental variables: water depth, SIC average and all seasonal SIC averages, SIC variability and all seasonal SIC variabilities, total SST average and all seasonal SST averages, total SST variability and all seasonal SST variabilities, distance to both the South American and Antarctica coast, distance to ice shelves. We examined pairwise correlation between these variables by calculating correlation matrices with the Spearman rank correlation coefficients with Hmisc::rcorr and corrplot::corrplot. From variables that were highly correlated with each other ($\rho > 0.75$), we chose only one of them to remove redundancy. The selected variables (depth, SIC average, SIC variability, winter, spring, and summer SIC variability, distance to coast and distance to ice shelves) were subjected to stepwise multicolinearity testing using variance inflation factors (VIF), where we removed the variable with the highest VIF and recalculated VIFs until all VIF values were smaller than five (indicating no multicolinearity between variables). The remaining noncollinear six variables for downstream analysis were water depth, SIC average, SIC variability, spring SIC variability, distance to ice shelves and distance to coast.

3.6. Ecological analysis

Functions of the vegan R package v 2.6-8 (Oksanen et al., 2022) were used to analyse alpha and beta-diversity patterns. Community alpha diversity was assessed using multiple metrics for all replicates. Shannon diversity was calculated on absolute reads and species richness on rarefied ASV tables (rarefied to 57,064, the lowest read count across PCR replicates).

Multivariate analysis of community composition variations (i.e. betadiversity) in relation to environmental variables was performed using Hellingertransformed read count data (aggregating replicates by summing reads per ASV), to compensate for uneven sequencing effort across samples. Nonmetric multidimensional scaling (NMDS) was performed with the function metaMDS using Bray-Curtis dissimilarities and two dimensions. The resulting NMDS was rotated so the x-axis was parallel to SIC average (function MDSrotate) for better visualization. A permutational multivariate analysis of variance (PERMANOVA, Anderson, 2001) was conducted on the same Hellinger-transformed read count data, using the adonis2 function and Bray-Curtis dissimilarities. We tested the visually separating clusters in the NMDS with 999 permutations. We also assessed marginal effects of the selected environmental variables with an additive model and 999 permutations. PERMANOVA by marginal terms assesses the single effects of the terms after accounting for all other terms in the model. We report the strength of the single effects of environmental variables (R^2) as well as the total variance explained by the model in % as (1 - residual R^2) * 100, which is the effect size of all single effects together with combined effects. We

also report the unbiased partial effect size ω^2 estimated using the MicEco package v0.10.0 (Russel, 2026), which is less influenced by sample size. We then used the envfit function and 999 permutations to fit the selected environmental variables to the NMDS ordination for a visual representation of the environmental variables in the two-dimensional NMDS space.

3.7. Total organic carbon

TOC contents of samples JR244/554, 562, 564, 566, 590, 591, 627, 628 and 639 were determined at the Alfred Wegener Institute in Bremerhaven. For this purpose, ~0.1 g of freeze-dried and homogenized sediment was decalcified with 500 µL hydrochloric acid and analysed by means of a carbonsulfur determinator (Eltra-CS800) following Lamping et al. (2021). Further TOC contents of the surface sediments originate from a published data set (Lamping et al., 2021).

3.8. Diatom abundances

A total of 19 smear slides were prepared for a quantitative diatom assemblage analysis of the surface sediments with a ZEISS AXIOPLAN II microscope at 1000× magnification. Between 133 and 636 diatom valves, including those from *Chaetoceros* resting spores, were counted in each sample for a subset of samples (PS111/139-2, 131-2, 98-3, 80-3, 42-1, 114-3, 70-2, 60-3, 47-2, 15-1, 16-3, 13-2, PS118/10-3, 12-2, 38-5, 62-3, 05-3, 48-2, 75-1). Diatoms were identified to species or species group level and, if possible, to forma or variety level. Following the taxonomy described by Armand and Zielinski (2001); Hasle and Syvertsen (1996); Zielinski and Gersonde (1997) we identified 33 different species, varieties or forma.

4. Results

Our metabarcoding approach generated initially a total of 66,550,397 sequences from 45 stations spanning diverse sea ice regimes. After processing with DADA2 (filtering, denoising, merging), removal of remaining sequences that contained primer sequence and removal of chimeras, 63,831,228 sequences (95.9%) remained. They were grouped into 63,945 ASVs and taxonomically assigned.

Contamination controls (sampling control, subsampling control, extraction control, PCR negative controls) contained low read counts (50,564 reads overall, with 533 reads on average per negative control reaction) predominantly of taxa that were expected in our study (i.e. marine plankton or benthic taxa). Therefore, we employed SCRuB to remove this low level of well-to-well leakage (see Appendix F for details on the decontamination). PCoA ordination based on Bray-Curtis dissimilarity confirmed that decontamination did not alter the main structure of eukaryotic communities (Appendix Fig. F.1).

After decontamination, additional filtering based on taxonomic annotations ensured that only high-quality eukaryotic sequences were retained for analysis. From the remaining 56,930,136 sequences (21,430 ASVs), we removed 3.9% of reads (3251 ASVs, 15.17% of ASVs) as non-eukaryotic ASVs. One PCR replicate with a low read number (<20,000) was excluded from downstream analysis. In total, 28.4% of unique ASVs (54,693,976 reads) were retained, classified into 18,144 eukaryotic ASVs distributed across 134 technical replicates ranging from 57 k to 810 k reads.

4.1. Overall taxonomic composition

Eukaryotic communities in surface sediments recovered 44 subdivisions but samples were dominated by diatoms and benthic taxa. Gyrista (mainly diatoms from the Mediophyceae and Bacillariophyceae classes) comprised over 32% of total reads (Fig. 2A), followed by

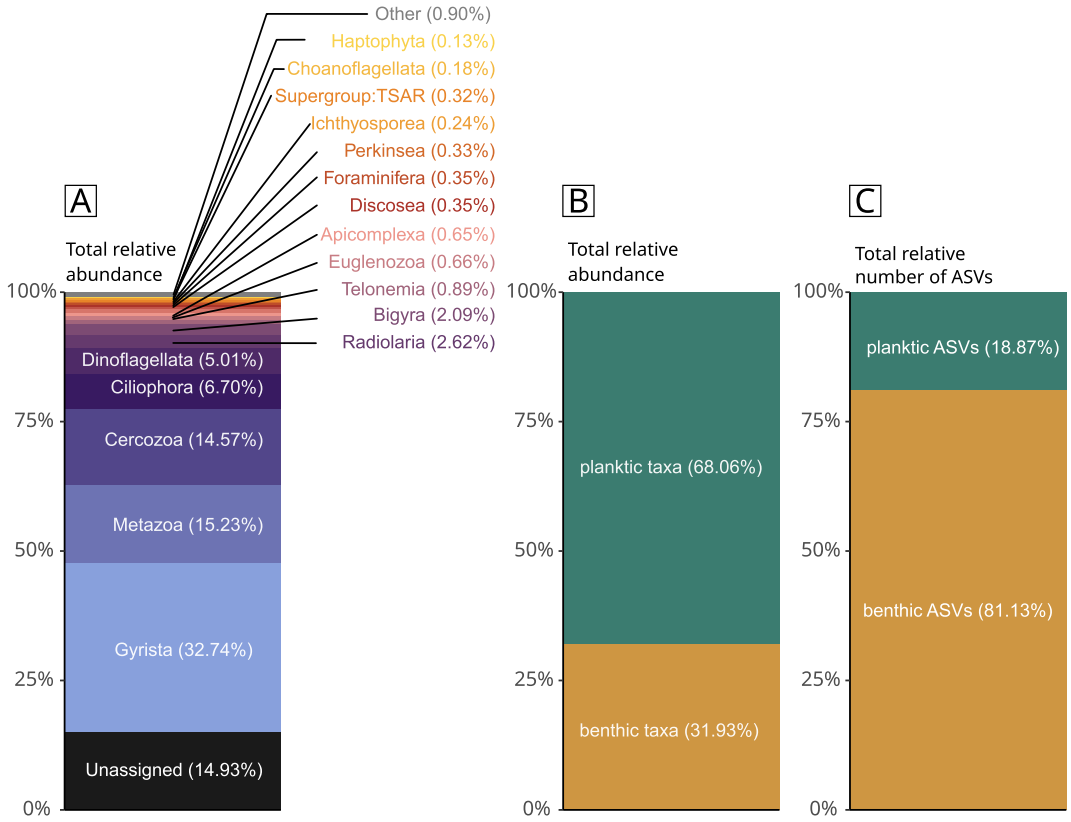

Fig. 2. A: Overall taxonomic composition of all stations in our dataset. Displayed are the relative abundances of the 20 most abundant taxa at the subdivision level. Other taxa were grouped into "Other". B: Relative abundance (% of reads) of planktic and benthic taxa. C: Relative number of planktic and benthic ASVs.

Metazoa (animals, 15%), Cercozoa (14.5%) and unassigned taxa (14.9%).

At the individual ASV level, extreme dominance of a few ASVs characterized the dataset. The two most abundant ASVs, both identified as Chaetocerotaceae diatoms, comprised over 20% and 3% of all reads respectively. The next most abundant ASVs belonged to benthic animals but were much less abundant: Nemertea (ribbon worms, 1.82% and 0.63%), Annelida (segmented worms, 1.13%, 0.98%), and Anthozoa (sea anemones, 0.98%).

Habitat annotation revealed contrasting patterns of abundance and diversity between planktic and benthic communities. Planktic taxa dominated eukaryotic communities with 68% of all reads whereas only 32% of all reads were assigned to benthic taxa (Fig. 2B). However, planktic taxa were much less diverse with only 3423 ASVs (18.87%), while benthic taxa accounted for 14,721 ASVs (81.13%, Fig. 2C).

4.2. Community composition across sea ice regimes

We examined the community composition in polynya-related regions (11 stations), perennial sea ice regions (15 stations), seasonal sea ice regions (12 stations) and open ocean regions (7 stations; see also Table 2 and Appendix Tables A.1 and B.2). We observed a slight increase in unassigned taxa and benthic taxa from the shelf towards the open ocean region (Fig. 3). Water depth at the stations in the polynya-related and perennial sea ice regions was shallower (329 to 1246 m and 332 to 1166 m, respectively) than in the other sea ice environments (seasonal sea ice region: 1405 to 4748 m; open ocean region: 2803 to 4172 m).

The shallower polynya-related and perennial sea ice regions are characterized by higher relative abundance of planktic taxa and a slightly higher TOC content, compared to the deeper seasonal and open ocean stations (Fig. 3 and Table 2), although there is no statistically significant difference of medians (Kruskal-Wallis p-value > 0.1, likely because of the small group sizes). In these shallower regions, Gyrista — dominated by Bacillariophyceae — are the most abundant subdivision, with their relative abundance decreasing from the polynya-related zone and perennial sea ice zone to the seasonal sea ice zone and open ocean zone (Table 2 and Fig. 3). In contrast, communities from the deeper regions are characterized by unassigned taxa, diatoms dominated by Mediophyceae and Crysophyceae, and Radiolaria (Fig. 3 and Appendix Fig. G.2), where unassigned taxa display an opposite abundance pattern

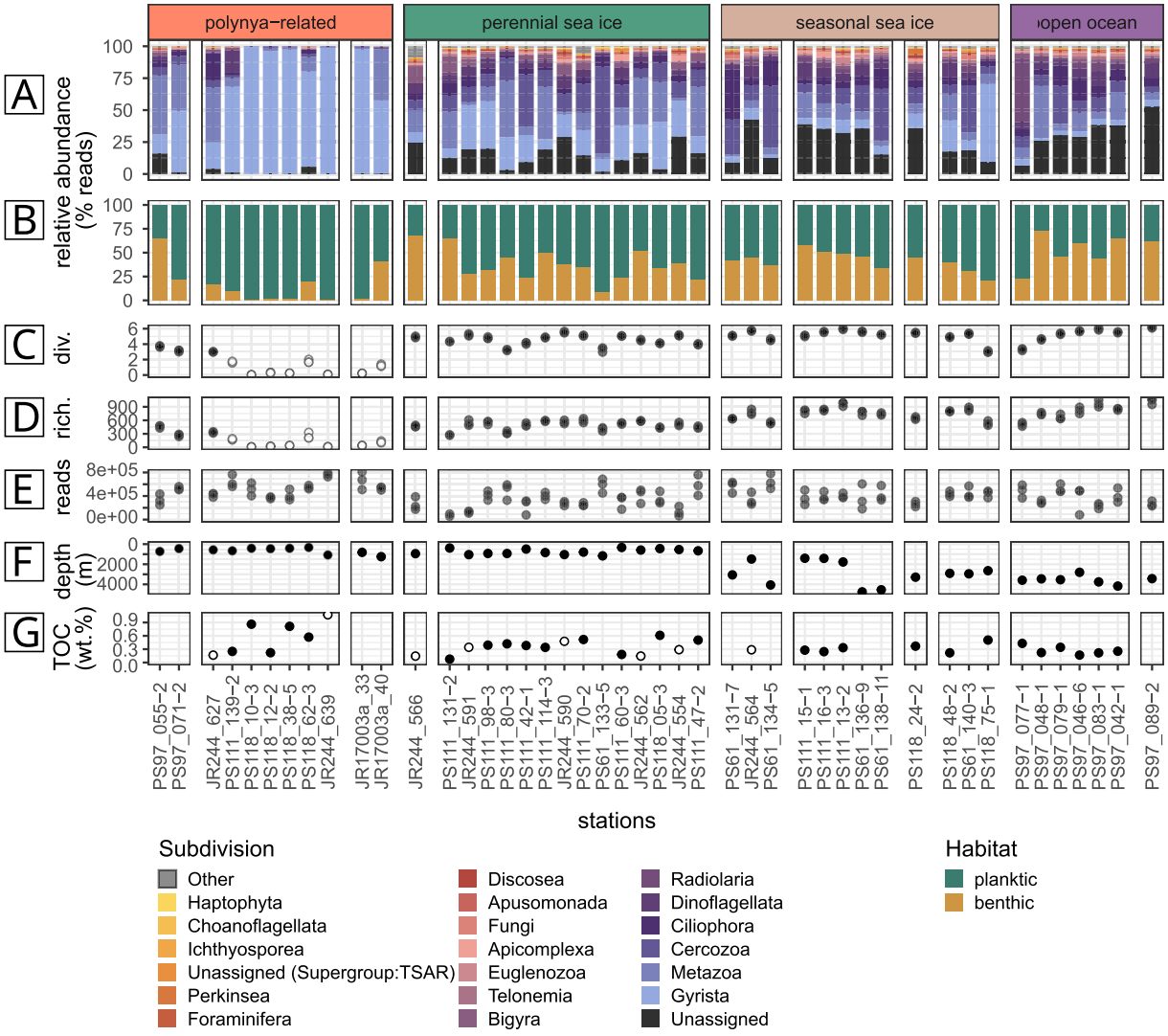

Fig. 3. Composition of eukaryotic communities across sea ice environments. The color code of the regions corresponds to the map (Fig. 1). A: taxonomic barplot showing relative abundance of the 20 most abundant taxa at the subdivision level. PCR replicates were aggregated per station. B: Relative abundance of planktic and benthic ASVs across all stations. C: Shannon diversity index for each technical replicate. Low-diversity stations excluded in statistical analysis highlighted by white fill. D: Rarefied ASV richness for each technical replicate. Low-diversity stations excluded in statistical analysis highlighted by white fill. E: Absolute reads for each technical replicate. F: Water depth at each station. G: TOC from (Lamping et al., 2021, black fill) and this study (white fill; Appendix Table C.3).

to Gyrista.

4.2.1. Polynya-related region

The analysis of community structures revealed that polynya-related environments harbored distinct communities compared to other sea ice regimes. We observed a dominance of Gyrista at the eight stations located in polynya-related regions around the Antarctic Peninsula and in front of the Brunt Ice shelf (Fig. 3). The communities from these stations comprised 50% to 99.5% of diatoms of the family Chaetocerotaceae, stemming almost entirely from one single ASV (Fig. 4). At five of these stations Chaetocerotaceae even dominated with >96% of reads. This high dominance of Chaetocerotaceae resulted in lower Shannon diversity values (mean of 0.7 and range of 0.03 to 2.01) compared to other samples in our dataset (mean 4.77, range 2.94 to 6.18).

Only three stations in polynya-related regions (out of eight) were not dominated by Chaetocerotaceae: PS97/71–2 and PS97/055-2 in the Bransfield Strait, as well as JR244/627 close to the Brunt Ice shelf. In samples from the Bransfield Strait, Annelida (segmented worms) and Maxillopoda (Crustaceans) were the most abundant metazoans, while the Gyrista consisted predominately of Bacillariophyceae (pennate diatoms) instead of Mediophyceae. In the sample collected close to the Brunt Ice shelf, the most abundant taxa were Nemertea (ribbon worms) and Ciliophora. The relative abundance of benthic taxa in the polynya-related region was generally below 22% but increased to ~40 and ~65%, at stations JR17003a/40 in the Prince Gustav Channel and PS97/055–2 in the Bransfield Strait, respectively.

4.2.2. Perennial sea ice region

The perennial sea ice region is characterized by substantially higher alpha diversity than the polynya regions, with a Shannon diversity ranging between ~3 and ~5 and a rarefied ASV richness between 272 and 593 (Fig. 3). In this region, Gyrista, Metazoa and Cercozoa are the most abundant subdivisions, contributing on average 21% (ranging from 7 to 37%), 19% (>1–44%), and 19% (7–67%) of reads, respectively, at single stations. Here, the Gyrista assemblage consists mainly of Bacillariophyceae and Mediophyceae. Planktic taxa contribute between 32% and over 90% of reads to the assemblage with an average of 62%. Unassigned ASVs represent on average ~15% of the reads. Water depth

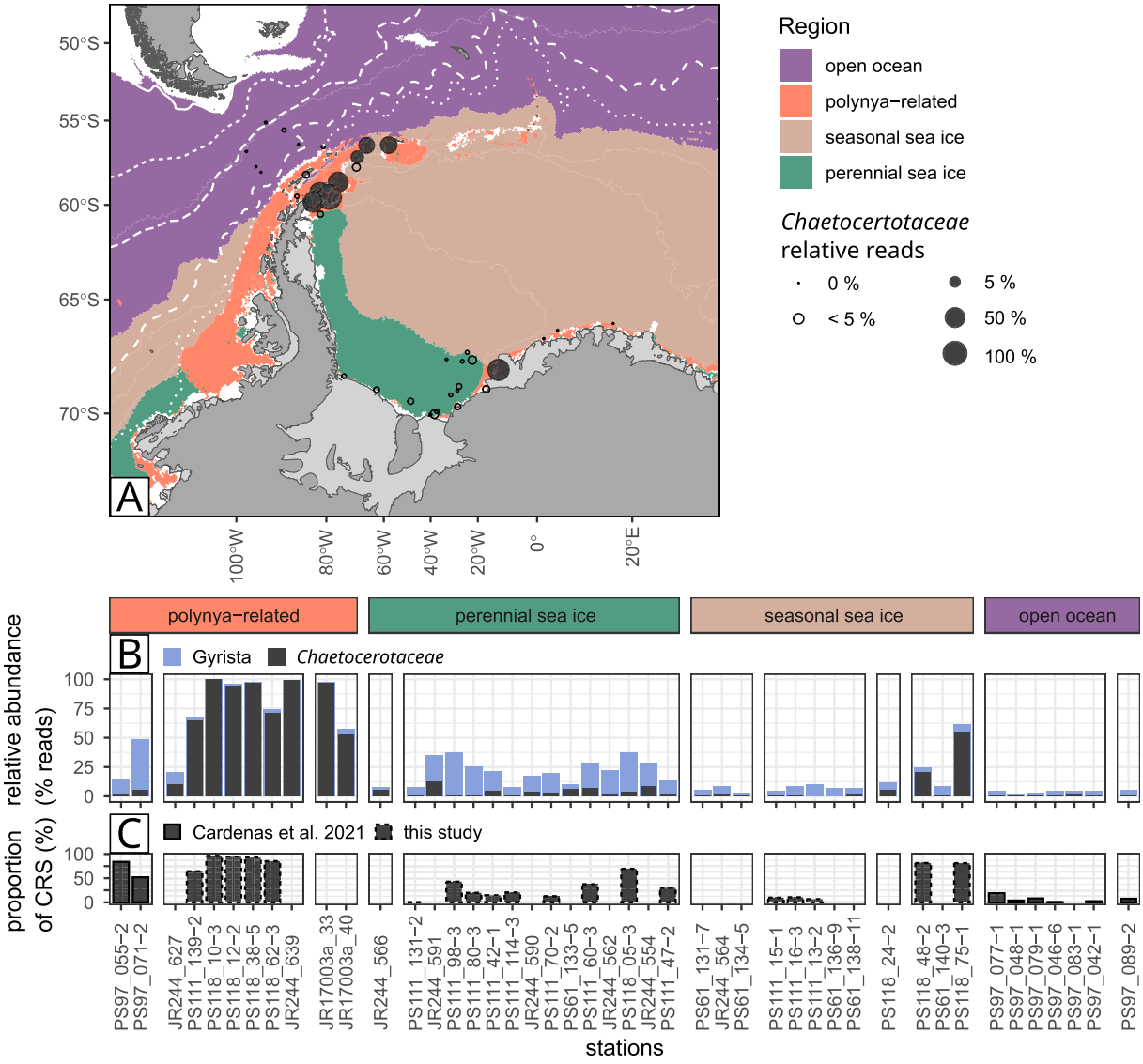

Fig. 4. High abundance of Chaetocerotaceae reads in polynya-related regions. A: Map showing relative abundances of Chaetocerotaceae as circles. Grey filled circles highlight sedimentary DNA communities with over 5% contribution of Chaetocerotaceae. Empty circles depict abundances below 5%. For all other map features Fig. 1. B: Relative abundance of reads assigned to family Chaetocerotaceae in the foreground (dark grey) and subdivision Gyrista in the background (light blue). C: Counts of *Chaetoceros* resting spores relative to other diatoms from Cárdenas et al. (2019, solid outline) and from this study (dashed outline). (For interpretation of the references to color in this figure legend, the reader is referred to the web version of this article.)

in the perennial sea ice region is comparable to the water depth in the polynya-related regions and relatively shallow (~330 to 1170 m).

4.2.3. Seasonal sea ice region

In the seasonal sea ice region, we found a slightly higher alpha diversity than in the perennial sea ice region (average Shannon diversity of 5.1 and a rarified ASV richness between 533 and 960 (Fig. 3)). Here, Cercozoa reach the highest relative abundance on average (20%), but it fluctuates considerably (5–50%) between stations, followed by Gyrista with on average 13% relative abundance (2–60%) and Ciliophora with an average of 10% (3–40%). On average 58% of reads were assigned to planktic taxa, fluctuating between ~40 to almost 80% at single stations. Metazoa contributed 9% on average but reached maximum relative abundances of 20%. The family Chaetocerotaceae also occurs in high relative abundances (two ASVs with over 50 and over 20%, respectively) at the northernmost stations in the Powell basin (PS118/75-1 and PS118/48-2), where seasonal sea ice is present with a SIC average of 27 to 39%. At all other stations, the contribution of Gyrista to the communities stays below 10% of the reads. This corresponds to stations with a SIC average over 50% (except station PS61/140 with a SIC average of 30%), where Chaetocerotaceae are nearly not detected. The contribution of unassigned ASVs is on average higher than in the perennial sea ice zone with 25% of the reads (9–42%). The stations in the seasonal sea ice region reach the deepest water depths with over 4500 m (PS61/136-9, 138-11).

4.2.4. Open ocean region

Highest alpha diversity is found in the open ocean region with an average Shannon index of 5.2 and rarified ASV richness between 512 and 1022 (Fig. 3). On average, Metazoa have the highest relative abundance with 14% of the reads (5–40%), followed by Cercozoa with 11% (5–30%), Radiolaria with 10% (2–50%) and Ciliophorea with 9% (4–17%). The open ocean region shows the least amount of contribution of planktic taxa with an average of 47%, fluctuating between 27 and 77%. Here, Gyrista do not reach above ~ 5% relative abundance. Unassigned ASVs contribute the most to this region with on average over 30% of the reads (6–52%). Water depth in the open ocean region is deep, ranging between 2800 and 4200 m.

4.3. Influence of environmental conditions on community composition

To avoid overwhelming signals from extreme Chaetocerotaceae dominance obscuring subtler community differences, we excluded the eight lowdiversity stations (Shannon diversity <2.1, Fig. 3) from multivariate analysis. This left us with three stations (PS97/71-2, PS97/055-2, JR244/627) from polynya-related regions.

NMDS with fitted environmental variables (Table 1, Appendix Table D.4) indicated that communities differed most between shallower samples with high SIC (perennial sea ice region and polynya-related region) and deeper samples with low SIC (seasonal sea ice and open ocean regions; Fig. 5). These two clusters (shallower vs. deeper samples) are significantly different ($p = 0.001$), explaining 16% (planktic community, $R^2 = 0.161$, $\omega^2 = 0.134$) or 11% (whole community, $R^2 = 0.109$, $\omega^2 = 0.082$) of the total variance in community composition in PERMANOVA.

Environmental variables explained 27.2% of the total variance in community compositions in a marginal PERMANOVA test. There was a small but significant ($p < 0.05$) effect of water depth ($R^2 = 0.045$, $\omega^2 = 0.022$), SIC average ($R^2 = 0.037$, $\omega^2 = 0.013$), and SIC variability ($R^2 = 0.034$, $\omega^2 = 0.010$) on sedimentary DNA communities. When only considering planktic taxa, the explained community variance increased (to 33.2%), as well as the importance of the significant variables water depth ($R^2 = 0.053$, $\omega^2 = 0.036$), SIC average ($R^2 = 0.040$, $\omega^2 = 0.022$), and SIC variability ($R^2 = 0.036$, $\omega^2 = 0.016$). In Fig. 5 the respective NMDS ordination is displayed showing the environmental variables significant in PERMANOVA.

4.4. Total organic carbon

TOC values in the polynya-related region reached maximum values of over 0.9 wt% at one station (JR244/639) and are above 0.5 wt% at three more stations (PS118/10–3, 38–5, 62–3). Three further stations are below 0.3 wt% (JR244/827, PS111/139–2, PS118/12–2). We did not retrieve TOC values from stations PS97/055–2 and 071–2 as well as JR17003a/33, and 40 (Appendix Table C.3 and Table 2). In the perennial sea ice region TOC values reach maxima of about 0.6 wt% (PS118/05-3) but stay generally between 0.29 and 0.52 wt%. Minima are ranging from 0.07 to 0.18 wt% (PS111/1312, 60–3, JR244/562, 566). We did not retrieve TOC values from station PS61/133-5. In the seasonal sea ice region TOC values reach a maximum of about 0.5wt.% (PS111/75-1) but otherwise stay between 0.2 and 0.4 wt%. We did not retrieve TOC values from stations PS61/131-7, 134-5, 136-9, 138-11 and 140-3. In the open ocean region TOC values reach maxima of about 0.3 and 0.4 wt.% (PS97/79-1 and 77-1) but otherwise stay relatively low between 0.2 and 0.3 wt.%. We did not retrieve TOC values from station PS97/89-2.

4.5. Chaetoceros resting spore abundance estimates

To estimate abundances of *Chaetoceros* resting spores across sea ice environments in the microfossil record, we combined new smear slide data from a subset of samples (see Section 3 material and methods) with previously published counts (Cárdenas et al., 2019, PS97/055-2, 071-2, 077-1, 048-1, 079-1, 046-6, 042-1, 089-1, Appendix Table C.3). We did not retrieve counts for samples from cruises JR244, JR17003a, PS61 and from PS118/242. The observed *Chaetoceros* specimens belong exclusively to the subgenus *Hyalochaetae*, mainly represented by resting spores. The resting spores have not been identified to species level due to the lack of distinguishable morphological features. Abundance of *Chaetoceros* resting spores relative to other diatoms was generally highest in polynya-related regions and lowest in open ocean regions. Relative abundances reached maxima of 84 to 96% at polynya-related

Table 1
PERMANOVA results. We tested six variables by marginal terms and report the R^2 (marginal (unique) contribution of each variable after accounting for all others), ω^2 (unbiased estimate of effect size), F-statistics and Pr(>F) (*p*-value) here. Total variance explained is reported in % (1 - residual R^2) * 100). Depth, SIC average and SIC variability are significant (p < 0.05, in bold) for both, whole (planktic and benthic) communities (left) as well as planktic communities only (right).

	Whole community				Planktic only			
	R^2	ω^2	F	Pr(>F)	R^2	ω^2	F	Pr(>F)
Water depth	0.045	0.022	1.845	**0.004**	0.053	0.036	2.385	**0.005**
SIC average	0.037	0.013	1.505	**0.019**	0.040	0.022	1.816	**0.016**
SIC variability	0.034	0.010	1.383	**0.047**	0.036	0.016	1.617	**0.041**
Spring SIC variability	0.029	0.006	1.216	0.099	0.031	0.010	1.391	0.084
Distance to coast	0.028	0.004	1.152	0.146	0.026	0.004	1.163	0.216
Distance to ice	0.028	0.005	1.172	0.135	0.029	0.008	1.312	0.114
Residual	0.728				0.668			
Total variance explained	27.2%				33.2%			

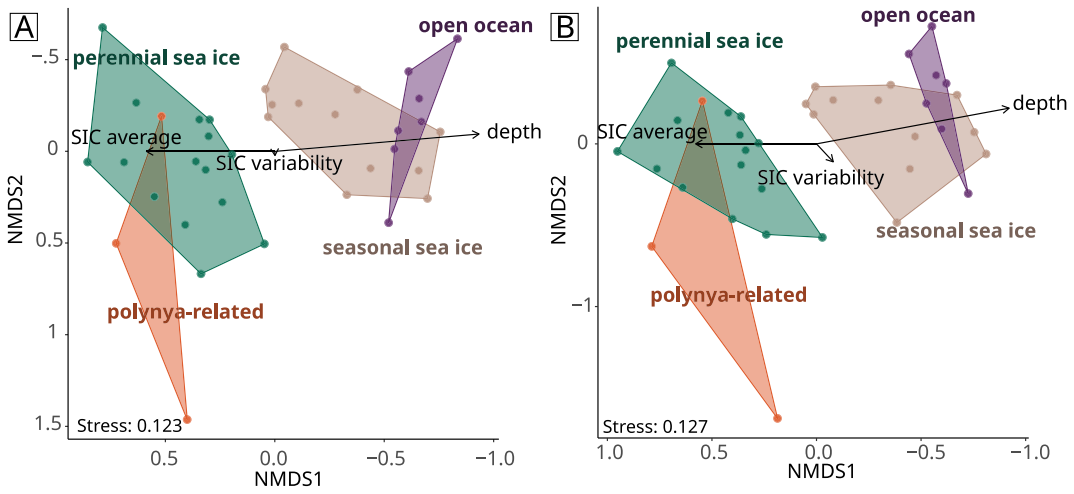

Fig. 5. NMDS ordinations showing sedimentary DNA community compositions for (A) all ASVs and (B) only planktic ASVs. Each point depicts the community profile of a station. Colored hulls depict the sea ice environments. Arrows indicate environmental variables significant in the PERMANOVA fitted to the NMDS ordination (function envfit). The length of the arrows depicts the goodness of fit (importance) of the respective variable to the NMDS ordination.

Table 2
Summary of group size, mean and standard deviation of relative planktic abundances and TOC content in the sea ice environments, after removing the Chaetocerotaceae dominated stations.

Region	rel. planktic abundance			TOC content		
	n	mean	sd	n	mean	sd
Polynya-related	3	0.66	0.27	1	0.17	–
Perennial sea ice	15	0.63	0.16	14	0.34	0.16
Seasonal sea ice	12	0.59	0.10	7	0.32	0.10
Open ocean	7	0.47	0.17	6	0.27	0.10

stations, 81% at two seasonal sea ice zone stations (PS118/48-2 and 75-1), 69% at one perennial sea ice station (PS118/05-3) and 19% in the open ocean region (PS97/077-1).

5. Discussion

Our metabarcoding analysis of Southern Ocean eukaryote communities in surface sediments enabled us to examine three key questions: (1) how communities vary across sea ice environments, (2) which environmental variables best explain community compositions, and (3) whether planktic or benthic community signals in surface sediments show stronger relationships with sea ice conditions.

Two patterns stood out: First, Chaetocerotaceae DNA dominates sediment samples in polynya regions, offering a clear molecular signature that is consistent with conventional microfossil work (Fig. 4). Second, variations in water depth and sea ice concentration (SIC) have a small but significant effect on community structures (Fig. 5, Table 1). We could not rank their importance as deep samples were always associated with lower sea ice concentration in our dataset. Nevertheless, our findings support the potential of sedaDNA for paleoenvironmental reconstructions.

5.1. Dominance of Chaetocerotaceae characterizes polynya environments

The dominance of Chaetocerotaceae diatoms around the Antarctic Peninsula and along the Weddell Sea coast display a clear relation to a specific sea ice environment, namely polynya-related regions (Fig. 4). Polynyas are characterized by phytoplankton blooms (Arrigo and van Dijken, 2003) and previous work has linked the high sedimentation of resting spores to high seasonal productivity due to a stratified shallow mixed layer depth after freshwater input during the spring melt (Leventer, 1991; Leventer et al., 1996). Spore formation and export to the seafloor is then triggered by nutrient depletion in this shallow upper water layer, an otherwise rare happening in the generally nutrient-rich Southern Ocean (Leventer, 1991).

We found that Chaetocerotaceae reads can comprise >96% (five stations) and > 50% (three stations) of the total reads in shallower (<1000 m) stations with low to moderate sea ice concentration (32–83%) in polynya-related regions. We also found elevated relative abundances of Chaetocerotaceae at the two northernmost stations in the Powell Basin (PS118/75-1: over 50% and PS118/48-2: over 20%). While these are classified as seasonal sea ice stations based on our approach (see Section 3.4), these stations could also be considered polynya-related as they are within ~10 to 15 km of polynya-related regions, making it likely that their surface waters can be considered polynya-related.

The high number of Chaetocerotaceae reads in our metabarcoding data is consistent with microscope-based observations from the surface sediments investigated in this study (Fig. 4) as well as previous studies in polynya-related regions. Elevated abundances of *Chaetoceros* resting spores were found in surface sediments (Cárdenas et al., 2019; Crosta et al., 1997; Świło et al., 2016) and in sediment traps (Leventer, 1991) in the coastal area around the northeastern Antarctic Peninsula, and in the southern Weddell Sea in front of the ice shelves, in particular the Brunt Ice shelf (Crosta et al., 1997). A spearman rank correlation reveals a strong, statistically significant positive monotonic relationship (ρ = 0.84, p = 1.602 × 10–6) between relative abundances of Chaetocerotaceae in the metabarcoding data, and relative *Chaetoceros* resting spores counts from this study and Cárdenas et al. (2019). This supports the conclusion that both, our metabarcoding data and traditional microscope-based observations, show a relation of Chaetocerotaceae to polynya-related regions.

In several samples we almost solely recovered Chaetocerotaceae DNA reads, which resulted in extremely low alpha diversity. This observation may reflect a high amount of Chaetocerotaceae sedimentary DNA compared to other DNA in those samples. However, since our DNA extraction protocol is also retrieving DNA from resting spores (Armbrecht et al., 2020), we rather may have retrieved intact DNA from Chaetocerotaceae spores. Intact DNA may be better PCR-amplified compared to other sedimentary DNA that consists of degraded extracellular DNA due to biotic or abiotic decay during transport to the seafloor or in the sediment (Torti et al., 2015). Either way, whether the high abundance of Chaetocerotaceae DNA in our samples is of extracellular sediment-bound origin or from intact cysts, it is indicative of high productivity and export related to the specific sea ice setting

around the Antarctic Peninsula and along the southern Weddell Sea coast.

Three stations in the polynya-related regions (PS97/071-2, PS97/055-2, JR244/627) are not dominated by Chaetocerotaceae. They are characterized by a high relative abundance of Metazoa and Gyrista (diatoms). Here, contrasting to the Chaetocerotaceae-dominated diatom communities, unassigned diatoms (PS97/071-2; JR244/627) or Bacillariophyceae (PS97/055-2) ASVs were dominant. We can only speculate on what might be driving this signal. One possibility is that the total abundance of *Chaetoceros* resting spores per g sediment is genuinely lower than at the Chaetocerotaceae dominated stations. Another explanation includes potential biases in DNA extraction related to sediment composition, but we do not have sufficient sedimentological data to support this. It is also possible that local environmental conditions were suboptimal for Chaetocerotaceae growth. For example, biomarker data indicates that station JR244/627 experienced a very high sea ice cover compared to the close-by PS111/139 (data not shown), possibly implying an expanded summer or spring ice cover and less meltwater production. In addition, stations PS97/055-2 and PS97/071-2 are the only stations in our study that are located in the Bransfield Strait where warm and fresh Bellingshausen Sea Water encounters cold and salty Weddell Sea Water (Sangrà et al., 2011; Vorrath et al., 2020). These local conditions (i.e. formation of eddies and upwelling processes at the Peninsula Front) may further limit Chaetocerotaceae growth.

All in all, sedimentary DNA captures the same pattern as more conventional diatom assemblage studies, which is promising for paleoenvironmental studies that aim to utilize sedimentary (ancient) DNA as a paleoenvironmental proxy.

5.2. Water depth and sea ice influence sedimentary DNA communities

Our statistical analyses of whole (planktic and benthic) and planktic-only communities from sediment samples that are not dominated by Chaetocerotaceae (Fig. 5 and Table 1) showed that variations in water depth and SIC (SIC average and SIC variability) explain part of the differences in community structure. Although effect sizes are small, they were significant despite limited sample size and high community dimensionality. Community composition separated into two main clusters, one that includes stations in shallower polynya-related and perennial sea ice regions with generally higher SIC, and another cluster including deeper, seasonal sea ice and open ocean regions with generally lower SIC (Fig. 5, PERMANOVA significant and explaining 11 to 16% of total variance). This pattern might be partly driven by differences in richness or TOC content (Fig. 3). For example, Learman et al. (2016) showed a correlation of distinct communities (between Antarctic Peninsula and West Antarctic Coast) with nutrient as well as organic matter content. They also noticed a consistently lower richness around the Antarctic Peninsula. However, their study does not include samples deeper than 820 m. In our study, water depth and SIC average were confounded due to the opportunistic sampling design: deep sites (>1400 m) were in open ocean or seasonally sea ice regions, while perennial ice samples were restricted to shallower shelf areas (<1250 m). This reflects the scarcity of available frozen sediment samples because of difficult access to the Weddell Sea due to harsh sea ice and weather conditions. Increasing statistical power and disentangling these effects will require substantially more samples, particularly from deep, permanently ice-covered areas and shallower, ice-free regions.

Linking whole communities to sea ice conditions assumes both, planktic and benthic, communities to reflect surface ocean conditions. This is a reasonable assumption given the ample evidence of pelagic-benthic coupling in the Southern Ocean evident from primary production pulses that build up foodbanks (e.g. Smith et al., 2006, 2012), high export of particular organic carbon in high latitudes (e.g. Buesseler, 1998), as well as varying benthic responses dependent on the type of lipid supply (e.g. Rembauville et al., 2018). Remarkably, statistical analysis on planktic-only sedimentary DNA communities is comparable to the whole communities analysis, with both, water depth and SIC average and variability having significant effects on the communities (Table 1). This outcome emphasizes the influence of sea ice on both, primary production and pelagic-benthic coupling (Wassmann et al., 2006). Planktic ASV reads contribute to almost 70% of the total sedimentary DNA community in our samples, confirming the observation of Cordier et al. (2022), who found higher relative pelagic DNA abundance towards higher latitudes. Given the dominance of planktic reads in this study, it is likely that the same environmental variables explaining beta diversity patterns would be identified for both planktic-only and whole communities.

Interestingly, the total explained variance is slightly higher when focusing on planktic-only communities (Fig. 5 and Table 1), indicating a closer link between the planktic community signal in sedimentary DNA with the tested environmental variables. This supports our hypothesis that planktic communities are more directly affected by surface ocean environments than benthic communities.

To separate our ASVs into planktic and benthic, we took advantage of global-scale plankton metabarcoding datasets produced by Tara Oceans (Sunagawa et al., 2020) and Malaspina consortia (Duarte, 2015; Obiol et al., 2020), complemented by a Southern Ocean survey (Flegontova et al., 2023), and surface sediment datasets (Cordier et al., 2022). However, there are limitations to this approach. For instance, only a fraction of our ASVs (65.6% overall) were also encountered in these public plankton datasets. The bulk of new ASVs in our dataset, considered here as benthic, represent rare taxa. This exemplifies our gap in knowledge of Southern Ocean biodiversity in particular, and in deep-ocean benthic biodiversity in general (Brandt et al., 2007). This is not unexpected as we are presenting one of the first metabarcoding datasets of eukaryotic communities in Southern Ocean surface sediments. Previous studies (Cordier et al., 2022; Pawlowski et al., 2011) included only few sampling stations in the Southern Ocean, or focused on meiobenthos (Brannock et al., 2018) or another genetic marker than in this study (Learman et al., 2016). Additionally, our annotation is not considering the arguably most important habitat in the Southern Ocean, the sea ice. To fully characterize the Southern Ocean's eukaryotic diversity, we would need to include the sympagic habitat as a third habitat type next to planktic and benthic. This requires incorporation of either existing metabarcoding data from sea ice samples (e.g. Hardge et al., 2017; Torstensson et al., 2015), or sampling of those environments. To our knowledge there is currently no 18S database with annotated sympagic organisms. This all stresses the importance of taxonomic work and increasing the knowledge about organism ecology and habitat to further our understanding of ecosystems in both the modern and past ocean.

6. Conclusion

Our metabarcoding analysis of 45 stations in and around the Weddell Sea spanning diverse sea ice regimes demonstrates that eukaryotic surface sedimentary DNA communities reflect contemporary sea ice conditions in the Southern Ocean through two broad patterns.

First, Chaetocerotaceae diatoms dominate polynya-related regions in our dataset, providing a clear molecular signature for these productive ice-marginal environments which corroborates conventional diatom assemblage work. The correspondence between surface sedimentary DNA and conventional diatom assemblage surveys shows the potential of using DNA of Chaetocerotaceae taxa as a robust proxy for highly productive conditions in downcore records, particularly valuable where microfossil preservation may be poor.

Beyond polynya-related regions, our model testing the effect of water depth, SIC and distances to coast and ice shelves explains 27–33% of community variance. While marginal effects of single environmental variables are small but significant, planktic-only sedimentary DNA communities are slightly better explained by the variation of these environmental variables, compared to whole (planktic and benthic) communities. This suggests that planktic-focused sedaDNA analyses

may be better suited to reconstruct past sea ice environments in the Southern Ocean. However, our opportunistic sampling design could not disentangle water depth from multiyear average sea ice effects. Targeted sampling of deep ice covered regions (deeper Weddell Basin) and shallow ice free areas (north of Antarctic Peninsula tip, South Sandwich and South Georgia Islands) would help to resolve this. An increase in samples is also needed to increase the probability of detecting a larger effect of the tested environmental variables.

This study establishes a modern baseline necessary for potentially applying sedaDNA to reconstruct Southern Ocean sea ice environments from the sediment record. When combined with conventional proxies, sedaDNA offers enhanced taxonomic resolution for reconstructing past biological communities and their responses to sea ice changes — a critical benefit for better understanding ecosystem dynamics during past climate transitions and projecting possible responses to future sea ice loss.

Acknowledgements

We acknowledge the captains, crews and scientific teams on the various cruises on board Research Vessel Polarstern and Royal Research Ship James Clark Ross: PS61, PS97 (GPF Grant AWI_PS97_01), PS111 (GPF Grant AWI_PS111_00), PS118 (GPF Grant AWI_PS118_04), JR244, JR17003a. We are thankful to Adrian Glover and Jan W. Pawlowski for contribution of frozen sediment samples from the JR17003a and PS61 expeditions. We thank Mandy Kuck, Kristine Steinsland, Lina Schätz and Amelie Nübel as well as the British Antarctic Survey (Victoria Peck, Paul Geissler) for their help with sampling. The sequencing service was provided by the Norwegian Sequencing Centre (www.sequencing.uio.no), a national technology platform hosted by the University of Oslo and supported by the "Functional Genomics" and "Infrastructure" programs of the Research Council of Norway and the Southeastern Regional Health Authorities. We thank Dr. Daniel Soule for providing writing feedback and revisions. We would also like to express our gratitude to Kuldeep More and one anonymous reviewer for their constructive reviews.

This study is part of the ARCHIE (Late Quaternary Antarctic Cryosphere Interactions) project, project 324287, funded by the Research Council of Norway.

CRediT authorship contribution statement

Nele M. Vollmar: Writing – review & editing, Writing – original draft, Visualization, Software, Methodology, Investigation, Formal analysis, Data curation, Conceptualization. **Agnes K. M. Weiner:** Writing – review & editing, Supervision, Conceptualization. **Katja Häkli:** Writing – review & editing, Resources, Investigation. **Miriam I. Brandt:** Writing – review & editing, Methodology. **Juliane Müller:** Writing – review & editing, Resources, Investigation. **Oliver Esper:** Investigation. **Thomas G. Dahlgren:** Writing – review & editing, Resources. **Claire S. Allen:** Writing – review & editing, Resources. **Tristan Cordier:** Writing – review & editing, Supervision, Resources, Methodology, Conceptualization. **Stijn De Schepper:** Writing – review & editing, Supervision, Methodology, Funding acquisition, Conceptualization.

Declaration of competing interest

The authors declare the following personal relationships which may be considered as potential competing interests:

Given his role as guest editor at the special issue "The invisible complement: using sedimentary ancient DNA (sedaDNA) to improve marine ecosystem reconstructions", Stijn De Schepper had no involvement in the peer review of this article and had no access to information regarding its peer review. Full responsibility for the editorial process for this article was delegated to another journal editor. The other authors declare that they have no known competing financial interests or personal relationships that could have appeared to influence the work reported in this paper.

Appendix A. Supplementary data

Supplementary data to this article can be found online at https://doi.org/10.1016/j.marmicro.2026.102591.

Data availability

Demultiplexed metabarcoding data is available at the European Nucleotide Archive (ENA) under accession number PRJEB104882

References

Amaral-Zettler, L.A., McCliment, E.A., Ducklow, H.W., Huse, S.M., 2009. A Method for studying protistan diversity using massively parallel sequencing of V9 hypervariable regions of small-subunit ribosomal RNA genes. PLoS One 4, e6372. https://doi.org/10.1371/journal.pone.0006372.

Anderson, P.S., 1993. Evidence for an Antarctic winter coastal polynya. Antarct. Sci. 5, 221–226. https://doi.org/10.1017/S0954102093000288.

Anderson, M.J., 2001. A new method for non-parametric multivariate analysis of variance. Austral. Ecol. 26, 32–46. https://doi.org/10.1111/j.1442-9993.2001.01070.pp.x.

Armand, L.K., Zielinski, U., 2001. Diatom species of the genus rhizosolenia from southern ocean sediments: distribution and taxonomic notes. Diatom Res. 16, 259–294. https://doi.org/10.1080/0269249X.2001.9705520.

Armbrecht, L.H., 2020. The potential of sedimentary ancient DNA to reconstruct past ocean ecosystems. Oceanography 33, 116–123.

Armbrecht, L., Herrando-Pérez, S., Eisenhofer, R., Hallegraeff, G.M., Bolch, C.J.S., Cooper, A., 2020. An optimized method for the extraction of ancient eukaryote DNA from marine sediments. Mol. Ecol. Resour. 20, 906–919. https://doi.org/10.1111/1755-0998.13162.

Arrigo, K.R., van Dijken, G.L., 2003. Phytoplankton dynamics within 37 Antarctic coastal polynya systems. J. Geophys. Res. Oceans 108. https://doi.org/10.1029/2002JC001739.

Austin, G.I., Park, H., Meydan, Y., Seeram, D., Sezin, T., Lou, Y.C., Firek, B.A., Morowitz, M.J., Banfield, J.F., Christiano, A.M., Pe'er, I., Uhlemann, A.C., Shenhav, L., Korem, T., 2023. Contamination source modeling with SCRuB improves cancer phenotype prediction from microbiome data. Nat. Biotechnol. 41, 1820–1828. https://doi.org/10.1038/s41587-023-01696-w.

Brandt, A., Gooday, A.J., Brandão, S.N., Brix, S., Brökeland, W., Cedhagen, T., Choudhury, M., Cornelius, N., Danis, B., De Mesel, I., Diaz, R.J., Gillan, D.C., Ebbe, B., Howe, J.A., Janussen, D., Kaiser, S., Linse, K., Malyutina, M., Pawlowski, J., Raupach, M., Vanreusel, A., 2007. First insights into the biodiversity and biogeography of the Southern Ocean deep sea. Nature 447, 307–311. https://doi.org/10.1038/nature05827.

Brannock, P.M., Learman, D.R., Mahon, A.R., Santos, S.R., Halanych, K.M., 2018. Meiobenthic community composition and biodiversity along a 5500 km transect of Western Antarctica: a metabarcoding analysis. Mar. Ecol. Prog. Ser. 603, 47–60.

Buesseler, K.O., 1998. The decoupling of production and particulate export in the surface ocean. Glob. Biogeochem. Cycles 12, 297–310. https://doi.org/10.1029/97GB03366.

Callahan, B.J., McMurdie, P.J., Rosen, M.J., Han, A.W., Johnson, A.J.A., Holmes, S.P., 2016. DADA2: High-resolution sample inference from Illumina amplicon data. Nat. Methods 13, 581–583. https://doi.org/10.1038/nmeth.3869.

Cárdenas, P., Lange, C.B., Vernet, M., Esper, O., Srain, B., Vorrath, M.E., Ehrhardt, S., Müller, J., Kuhn, G., Arz, H.W., Lembke-Jene, L., Lamy, F., 2019. Biogeochemical proxies and diatoms in surface sediments across the Drake Passage reflect oceanic domains and frontal systems in the region. Prog. Oceanogr. 174, 72–88. https://doi.org/10.1016/j.pocean.2018.10.004.

Clarke, L.J., Bestley, S., Bissett, A., Deagle, B.E., 2019. A globally distributed Syndiniales parasite dominates the Southern Ocean microeukaryote community near the sea-ice edge. ISME J. 13, 734–737. https://doi.org/10.1038/s41396-018-0306-7.

Coolen, M.J., Gibson, J.A., 2009. Ancient DNA in lake sediment records. PAGES News 17, 104–106. https://doi.org/10.22498/pages.17.3.104.

Cordier, T., 2024. fastqUtils: Set of Functions to Demultiplex Illumina Amplicon Libraries and Running the dada2 Workflow. Version 0.1.0, #7c935ea. https://github.com/trtcrd/fastqUtils.

Cordier, T., Angeles, I.B., Henry, N., Lejzerowicz, F., Berney, C., Morard, R., Brandt, A., Cambon-Bonavita, M.A., Guidi, L., Lombard, F., Arbizu, P.M., Massana, R., Orejas, C., Poulain, J., Smith, C.R., Wincker, P., Arnaud-Haond, S., Gooday, A.J., de Vargas, C., Pawlowski, J., 2022. Patterns of eukaryotic diversity from the surface to the deep-ocean sediment. Sci. Adv. 8, eabj9309. https://doi.org/10.1126/sciadv.abj9309.

Crosta, X., Pichon, J.J., Labracherie, M., 1997. Distribution of Chaetoceros resting spores in modern peri-Antarctic sediments. Mar. Micropaleontol. 29, 283–299. https://doi.org/10.1016/S0377-8398(96)00033-3.

Crosta, X., Kohfeld, K.E., Bostock, H.C., Chadwick, M., Du Vivier, A., Esper, O., Etourneau, J., Jones, J., Leventer, A., Müller, J., Rhodes, R.H., Allen, C.S., Ghadi, P., Lamping, N., Lange, C.B., Lawler, K.A., Lund, D., Marzocchi, A., Meissner, K.J., Menviel, L., Nair, A., Patterson, M., Pike, J., Prebble, J.G., Riesselman, C.,

Sadatzki, H., Sime, L.C., Shukla, S.K., Thöle, L., Vorrath, M.E., Xiao, W., Yang, J., 2022. Antarctic sea ice over the past 130 000 years – part 1: a review of what proxy records tell us. Clim. Past 18, 1729–1756. https://doi.org/10.5194/cp-18-1729-2022.

De La Rocha, C.L., Passow, U., 2007. Factors influencing the sinking of POC and the efficiency of the biological carbon pump. Deep Sea Res. II 54, 639–658. https://doi.org/10.1016/j.dsr2.2007.01.004.

De Schepper, S., Ray, J.L., Skaar, K.S., Sadatzki, H., Ijaz, U.Z., Stein, R., Larsen, A., 2019. The potential of sedimentary ancient DNA for reconstructing past sea ice evolution. ISME J. 13, 2566–2577. https://doi.org/10.1038/s41396-019-0457-1.

Deppeler, S.L., Davidson, A.T., 2017. Southern ocean phytoplankton in a changing climate. Front. Mar. Sci. 4. https://doi.org/10.3389/fmars.2017.00040.

Dorschel, B., 2019. The Expedition PS118 of the Research Vessel POLARSTERN to the Weddell Sea in 2019. Technical Report. AlfredWegener-Institut, Helmholtz-Zentrum für Polar- und Meeresforschung. https://doi.org/10.2312/BZPM_0735_2019.

Duarte, C.M., 2015. Seafaring in the 21St century: the Malaspina 2010 circumnavigation expedition. Limnol. Oceanogr. Bull. 24, 11–14. https://doi.org/10.1002/lob.10008.

Ducklow, H., Steinberg, D., Buesseler, K., 2001. Upper ocean carbon export and the biological pump. Oceanography 14, 50–58. https://doi.org/10.5670/oceanog.2001.06.

Dufresne, Y., Lejzerowicz, F., Perret-Gentil, L.A., Pawlowski, J., Cordier, T., 2019. SLIM: a flexible web application for the reproducible processing of environmental DNA metabarcoding data. BMC Bioinformatics 20, 88. https://doi.org/10.1186/s12859-019-2663-2.

Ellegaard, M., Clokie, M.R.J., Czypionka, T., Frisch, D., Godhe, A., Kremp, A., Letarov, A., McGenity, T.J., Ribeiro, S., John Anderson, N., 2020. Dead or alive: sediment DNA archives as tools for tracking aquatic evolution and adaptation. Commun. Biol. 3, 169. https://doi.org/10.1038/s42003-020-0899-z.

Epp, L.S., Zimmermann, H.H., Stoof-Leichsenring, K.R., 2019. Sampling and extraction of ancient DNA from sediments. In: Shapiro, B., Barlow, A., Heintzman, P.D., Hofreiter, M., Paijmans, J.L.A., Soares, A.E.R. (Eds.), Ancient DNA, 1963. Springer New York, New York, NY, pp. 31–44. https://doi.org/10.1007/978-1-4939-9176-1_5.

Fitter, K., Guillaumot, C., Ranzolin, D., Desgroseilliers, M., Raymond, B., 2025. quantarcticR: Access to Quantarctica Data Sets.

Flegontova, O., Flegontov, P., Jachníková, N., Lukeš, J., Horák, A., 2023. Water masses shape pico-nano eukaryotic communities of the Weddell Sea. Commun. Biol. 6, 1–10. https://doi.org/10.1038/s42003-023-04452-7.

Fütterer, D.K., Brandt, A., Poore, G.C.B., 2003. The Expeditions ANTARKTIS-XIX/3–4 of the Research Vessel POLARSTERN in 2002 (ANDEEP I and II: Antarctic Benthic Deep-Sea Biodiversity - Colonization History and Recent Community Patterns). Technical Report. Alfred-Wegener-Institut für Polar- und Meeresforschung. https://doi.org/10.2312/BZPM_0470_2003.

GEBCO Bathymetric Compilation Group, 2023. The GEBCO_2023 Grid - A Continuous Terrain Model of the Global Oceans and Land. https://doi.org/10.5285/F98B053B-0CBC-6C23-E053-6C86ABC0AF7B.

Geraldi, N.R., Krause-Jensen, D., Ørberg, S.B., Frühe, L., Sejr, M.K., Hansen, J.L.S., Lund-Hansen, L., Duarte, C.M., 2024. Environmental drivers of Arctic communities based on metabarcoding of marine sediment eDNA. Proc. R. Soc. B Biol. Sci. 291, 20231614. https://doi.org/10.1098/rspb.2023.1614.

Grimes, C.J., Mahon, A.R., Donnelly, K.B., Farris, W., Gott, M., Halanych, C., Judge, C., Mancke, H.I., Noor, N.J., Schreiter, S.A., Uzarski, L., Zehnpfennig, J.R., Halanych, K. M., 2025. Benthic community heterogeneity on the Eastern Antarctic continental shelf. Polar Biol. 48, 35. https://doi.org/10.1007/s00300-025-03354-0.

Guillou, L., Bachar, D., Audic, S., Bass, D., Berney, C., Bittner, L., Boutte, C., Burgaud, G., de Vargas, C., Decelle, J., del Campo, J., Dolan, J.R., Dunthorn, M., Edvardsen, B., Holzmann, M., Kooistra, W.H., Lara, E., Le Bescot, N., Logares, R., Mahé, F., Massana, R., Montresor, M., Morard, R., Not, F., Pawlowski, J., Probert, I., Sauvadet, A.L., Siano, R., Stoeck, T., Vaulot, D., Zimmermann, P., Christen, R., 2013. The Protist Ribosomal Reference database (PR2): a catalog of unicellular eukaryote Small Sub-Unit rRNA sequences with curated taxonomy. Nucleic Acids Res. 41, D597–D604. https://doi.org/10.1093/nar/gks1160.

Hardge, K., Peeken, I., Neuhaus, S., Lange, B.A., Stock, A., Stoeck, T., Weinisch, L., Metfies, K., 2017. The importance of sea ice for exchange of habitat-specific protist communities in the Central Arctic Ocean. J. Mar. Syst. 165, 124–138. https://doi.org/10.1016/j.jmarsys.2016.10.004.

Hasle, G.R., Syvertsen, E.E., 1996. Chapter 2 - marine diatoms. In: Tomas, C.R. (Ed.), Identifying Marine Phytoplankton. Academic Press, San Diego, pp. 5–385.

Hijmans, R.J., 2023. Raster: Geographic Data Analysis and Modeling.

Huang, B., Liu, C., Banzon, V., Freeman, E., Graham, G., Hankins, B., Smith, T., Zhang, H. M., 2021. Improvements of the Daily Optimum Interpolation Sea Surface Temperature (DOISST) Version 2.1. https://doi.org/10.1175/JCLI-D-20-0166.1.

Hugerth, L.W., Andersson, A.F., 2017. Analysing microbial community composition through amplicon sequencing: from sampling to hypothesis testing. Front. Microbiol. 8, 1561. https://doi.org/10.3389/fmicb.2017.01561.

Iversen, M.H., 2023. Carbon export in the ocean: a biologist's perspective. Annu. Rev. Mar. Sci. 15, 357–381. https://doi.org/10.1146/annurev-marine-032122-035153.

Klinck, J., Nowlin, W.D., 2001. Antarctic Circumpolar Current. In: Encyclopedia of Ocean Sciences. Elsevier, pp. 151–159. https://doi.org/10.1006/rwos.2001.0370.

Koch, C.W., Brown, T.A., Amiraux, R., Ruiz-Gonzalez, C., MacCorquodale, M., Yunda-Guarin, G.A., Kohlbach, D., Loseto, L.L., Rosenberg, B., Hussey, N.E., Ferguson, S.H., Yurkowski, D.J., 2023. Year-round utilization of sea ice-associated carbon in Arctic ecosystems. Nat. Commun. 14, 1964. https://doi.org/10.1038/s41467-023-37612-8.

Kusahara, K., Williams, G.D., Tamura, T., Massom, R., Hasumi, H., 2017. Dense shelf water spreading from Antarctic coastal polynyas to the deep Southern Ocean: a regional circumpolar model study. J. Geophys. Res. Oceans 122, 6238–6253. https://doi.org/10.1002/2017JC012911.

Lamping, N., Müller, J., Hefter, J., Mollenhauer, G., Haas, C., Shi, X., Vorrath, M.E., Lohmann, G., Hillenbrand, C.D., 2021. Evaluation of lipid biomarkers as proxies for sea ice and ocean temperatures along the Antarctic continental margin. Clim. Past 17, 2305–2326. https://doi.org/10.5194/cp-17-2305-2021.

Lamy, F., 2016. The Expedition PS97 of the Research Vessel POLARSTERN to the Drake Passage in 2016. Technical Report. Alfred-Wegener-Institut, Helmholtz-Zentrum für Polar- und Meeresforschung. https://doi.org/10.2312/BZPM_0701_2016.

Larter, R.D., Allen, C.S., Gales, J.A., Graham, A.G.C., Hillenbrand, C.D., Hodgson, D.A., Østerhus, S., Peck, V.L., Preston, M., Robinson, M., Robst, J., Ruhnau, M., Smith, J., Sprenk, D., Wagner, J., 2011. JR244 Cruise Report, RRS James Clark Ross, Marine Geoscience and Physical Oceanography, Southern Weddell Sea and South Orkney Continental Shelf, January–March 2011. Technical Report. British Antarctic Survey.

Learman, D.R., Henson, M.W., Thrash, J.C., Temperton, B., Brannock, P.M., Santos, S.R., Mahon, A.R., Halanych, K.M., 2016. Biogeochemical and microbial variation across 5500 km of Antarctic surface sediment implicates organic matter as a driver of benthic community structure. Front. Microbiol. 7. https://doi.org/10.3389/fmicb.2016.00284.

Leventer, A., 1991. Sediment trap diatom assemblages from the northern Antarctic Peninsula region. Deep Sea Research Part a. Oceanogr. Res. Pap. 38, 1127–1143. https://doi.org/10.1016/0198-0149(91)90099-2.

Leventer, A., Domack, E.W., Ishman, S.E., Brachfeld, S., McClennen, C.E., Manley, P., 1996. Productivity cycles of 200–300 years in the Antarctic Peninsula region: Understanding linkages among the sun, atmosphere, oceans, sea ice, and biota. Geol. Soc. Am. Bull. 108, 1626–1644. https://doi.org/10.1130/0016-7606(1996)108<1626:pcoyit>2.3.co;2.

Linse, K., scientists of Larsen-C Benthos, February– - March 2018, 2026. JR17003a Cruise Report RRS James Clark Ross. British Antarctic Survey Cruise Report. British Antarctic Survey. Falkland Islands, Eastern Antarctic Peninsula, Prince Gustav Channel.

Maschette, D., Sumner, M., Raymond, B., 2019. SOmap: Southern Ocean Maps.

Massom, R.A., Scambos, T.A., Bennetts, L.G., Reid, P., Squire, V.A., Stammerjohn, S.E., 2018. Antarctic ice shelf disintegration triggered by sea ice loss and ocean swell. Nature 558, 383–389. https://doi.org/10.1038/s41586-018-0212-1.

Mayers, K.M.J., Vollmar, N.M., Cordier, T., Weiner, A.K.M., Müller, J., Larsen, A., De Schepper, S., 2026. First-year sea ice history in the Arctic Ocean inferred from ancient DNA of Polerella glacialis over the past 50,000 years. Earth Planet. Sci. Lett. 678, 119809. https://doi.org/10.1016/j. epsl.2025.119809.

Meier, W., Fetterer, F., Windnagel, A., Stewart, S., 2021. NOAA/NSIDC climate Data Record of Passive Microwave Sea Ice Concentration, Version 4. https://doi.org/10.7265/EFMZ-2T65.

Morales Maqueda, M.A., Willmott, A.J., Biggs, N.R.T., 2004. Polynya dynamics: a review of observations and modeling. Rev. Geophys. 42, 2002RG000116. https://doi.org/10.1029/2002RG000116.

Morard, R., Lejzerowicz, F., Darling, K.F., Lecroq-Bennet, B., Winther Pedersen, M., Orlando, L., Pawlowski, J., Mulitza, S., de Vargas, C., Kucera, M., 2017. Planktonic foraminifera-derived environmental DNA extracted from abyssal sediments preserves patterns of plankton macroecology. Biogeosciences 14, 2741–2754. https://doi.org/10.5194/bg-14-2741-2017.

Mormède, S., Irisson, J.O., Raymond, B., 2014. Distribution Modelling. In: De Broyer, C., Koubbi, P., Griffiths, H., Raymond, B., d'Udekem d'Acoz, C., Van de Putte, A., Danis, B., David, B., Grant, S., Gutt, J., Held, C., Hosie, G., Huettmann, F., Post, A., Ropert-Coudert, Y. (Eds.), Biogeographic Atlas of the Southern Ocean. Scientific Committee on Antarctic Research, Cambridge UK, pp. 27–29.

Obiol, A., Giner, C.R., Sánchez, P., Duarte, C.M., Acinas, S.G., Massana, R., 2020. A metagenomic assessment of microbial eukaryotic diversity in the global ocean. Mol. Ecol. Resour. 20, 718–731. https://doi.org/10.1111/1755-0998.13147.

Oksanen, J., Simpson, G.L., Blanchet, F.G., Kindt, R., Legendre, P., Minchin, P.R., O'Hara, R., Solymos, P., Stevens, M.H.H., Szoecs, E., Wagner, H., Barbour, M., Bedward, M., Bolker, B., Borcard, D., Carvalho, G., Chirico, M., De Caceres, M., Durand, S., Evangelista, H.B.A., FitzJohn, R., Friendly, M., Furneaux, B., Hannigan, G., Hill, M.O., Lahti, L., McGlinn, D., Ouellette, M.H., Ribeiro Cunha, E., Smith, T., Stier, A., Ter Braak, C.J., Weedon, J., 2022. Vegan: Community Ecology Package.

Ørberg, S.B., Krause-Jensen, D., Geraldi, N.R., Ortega, A., Díaz-Rúa, R., Duarte, C.M., 2022. Fingerprinting Arctic and North Atlantic Macroalgae with eDNA – application and perspectives. Environ. DNA 4, 385–401. https://doi.org/10.1002/edn3.262.

Orsi, A.H., Whitworth, T., Nowlin, W.D., 1995. On the meridional extent and fronts of the Antarctic Circumpolar Current. Deep-Sea Res. I 42, 641–673. https://doi.org/10.1016/0967-0637(95)00021-W.

Park, Y.H., Park, T., Kim, T.W., Lee, S.H., Hong, C.S., Lee, J.H., Rio, M.H., Pujol, M.I., Ballarotta, M., Durand, I., Provost, C., 2019. Observations of the Antarctic circumpolar current over the Udintsev fracture zone, the narrowest choke point in the southern ocean. J. Geophys. Res. Oceans 124, 4511–4528. https://doi.org/10.1029/2019JC015024.

Pawlowski, J., Christen, R., Lecroq, B., Bachar, D., Shahbazkia, H.R., Amaral-Zettler, L., Guillou, L., 2011. Eukaryotic richness in the abyss: insights from pyrotag sequencing. PloS One 6, e18169. https://doi.org/10.1371/journal.pone.0018169.

R Core Team, 2023. R: A Language and Environment for Statistical Computing (Vienna, Austria).

Raymond, B., 2014. Pelagic regionalisation. In: De Broyer, C., Koubbi, P., Griffiths, H., Raymond, B., d'Udekem d'Acoz, C., Van de Putte, A., Danis, B., David, B., Grant, S., Gutt, J., Held, C., Hosie, G., Huettmann, F., Post, A., Ropert-Coudert, Y. (Eds.), Biogeographic Atlas of the Southern Ocean. Scientific Committee on Antarctic Research, Cambridge UK, pp. 418–421.

Rembauville, M., Blain, S., Manno, C., Tarling, G., Thompson, A., Wolff, G., Salter, I., 2018. The role of diatom resting spores in pelagic–benthic coupling in the Southern Ocean. Biogeosciences 15, 3071–3084. https://doi.org/10.5194/bg-15-3071-2018.

Roach, L.A., Meier, W.N., 2025. Sea ice in 2024. Nat. Rev. Earth Environ. 6, 252–254. https://doi.org/10.1038/s43017-025-00662-1.

Russel, J., 2026. MicEco: Various Functions for Microbial Community Data.

Sangrà, P., Gordo, C., Hernández-Arencibia, M., Marrero-Díaz, A., Rodríguez-Santana, A., Stegner, A., Martínez-Marrero, A., Pelegrí, J.L., Pichon, T., 2011. The Bransfield current system. Deep-Sea Res. I Oceanogr. Res. Pap. 58, 390–402. https://doi.org/10.1016/j.dsr.2011. 01.011.

Schröder, M., 2018. The Expedition PS111 of the Research Vessel POLARSTERN to the Southern Weddell Sea in 2018. Technical Report. Alfred-Wegener-Institut, Helmholtz-Zentrum für Polar- und Meeresforschung. https://doi.org/10.2312/BZPM_0718_2018.

Smith, C.R., Mincks, S., DeMaster, D.J., 2006. A synthesis of bentho-pelagic coupling on the Antarctic shelf: food banks, ecosystem inertia and global climate change. Deep-Sea Res. II 53, 875–894. https://doi.org/10.1016/j.dsr2.2006.02.001.

Smith, C., DeMaster, D., Thomas, C., Srsen, P., Grange, L., Evrard, V., DeLeo, F., 2012. Pelagic-Benthic coupling, food banks, and climate change on the West Antarctic Peninsula shelf. Oceanography 25, 188–201. https://doi.org/10.5670/oceanog.2012.94.

Sokolov, S., Rintoul, S.R., 2009. Circumpolar structure and distribution of the Antarctic Circumpolar Current fronts: 1. Mean circumpolar paths. J. Geophys. Res. Oceans 114. https://doi.org/10.1029/2008JC005108.

Stark, J.S., Raymond, T., Deppeler, S.L., Morrison, A.K., 2019. Chapter 1 - Antarctic seas. In: Sheppard, C. (Ed.), World Seas: An Environmental Evaluation, Second edition. Academic Press, pp. 1–44. https://doi.org/10.1016/B978-0-12-805068-2.00002-4.

Sunagawa, S., Acinas, S.G., Bork, P., Bowler, C., Eveillard, D., Gorsky, G., Guidi, L., Iudicone, D., Karsenti, E., Lombard, F., Ogata, H., Pesant, S., Sullivan, M.B., Wincker, P., de Vargas, C., 2020. Tara Oceans: towards global ocean ecosystems biology. Nat. Rev. Microbiol. 18, 428–445. https://doi.org/10.1038/s41579-020-0364-5.

Świło, M., Majewski, W., Totten, R.L., Anderson, J.B., 2016. Diatom assemblages from coastal settings of West Antarctica. Mar. Micropaleontol. 125, 95–109. https://doi.org/10.1016/j.marmicro.2016.04.001.

Taberlet, P., Coissac, E., Hajibabaei, M., Rieseberg, L.H., 2012. Environmental DNA. Mol. Ecol. 21, 1789–1793. https://doi.org/10.1111/j.1365-294X.2012.05542.x.

Taberlet, P., Bonin, A., Zinger, L., Coissac, E., 2018. Environmental DNA: For Biodiversity Research and Monitoring, First edition ed. vol. 1. Oxford University Press, Oxford, United Kingdom. https://doi.org/10.1093/oso/9780198767220.001.0001.

Torstensson, A., Dinasquet, J., Chierici, M., Fransson, A., Riemann, L., Wulff, A., 2015. Physicochemical control of bacterial and protist community composition and diversity in Antarctic sea ice. Environ. Microbiol. 17, 3869–3881. https://doi.org/10.1111/1462-2920.12865.

Torti, A., Lever, M.A., Jørgensen, B.B., 2015. Origin, dynamics, and implications of extracellular DNA pools in marine sediments. Mar. Genomics 24, 185–196. https://doi.org/10.1016/j.margen.2015.08.007.

Vihtakari, M., 2022. ggOceanPlots: Helpers for the Analysis of Oceanographic Data.

Vorrath, M.E., Müller, J., Rebolledo, L., Cárdenas, P., Shi, X., Esper, O., Opel, T., Geibert, W., Muñoz, P., Haas, C., Kuhn, G., Lange, C.B., Lohmann, G., Mollenhauer, G., 2020. Sea ice dynamics in the Bransfield Strait, Antarctic Peninsula, during the past 240 years: a multi-proxy intercomparison study. Clim. Past 16, 2459–2483. https://doi.org/10.5194/cp-16-2459-2020.

Wassmann, P., Reigstad, M., Haug, T., Rudels, B., Carroll, M.L., Hop, H., Gabrielsen, G. W., Falk-Petersen, S., Denisenko, S.G., Arashkevich, E., Slagstad, D., Pavlova, O., 2006. Food webs and carbon flux in the Barents Sea. Prog. Oceanogr. 71, 232–287. https://doi.org/10.1016/j.pocean.2006. 10.003.

Zielinski, U., Gersonde, R., 1997. Diatom distribution in Southern Ocean surface sediments (Atlantic sector): implications for paleoenvironmental reconstructions. Palaeogeogr. Palaeoclimatol. Palaeoecol. 129, 213–250. https://doi.org/10.1016/S0031-0182(96)00130-7.

Zinger, L., Lionnet, C., Benoiston, A.S., Donald, J., Mercier, C., Boyer, F., 2021. metabaR: an R package for the evaluation and improvement of DNA metabarcoding data quality. Methods Ecol. Evol. 12, 586–592. https://doi.org/10.1111/2041-210X.13552.